Optical properties of PZT thin films deposited on a ZnO buffer layer.

T. Schneider, D. Leduc, J. Cardin, C. Lupi, N. Barreau⋆ and H. Gundel

Université de Nantes, Nantes Atlantique Universités, IREENA, EA1770, Faculté des Sciences et des Techniques, 2 rue de la Houssinière - BP 9208, Nantes, F-44000 France.

⋆Université de Nantes, Nantes Atlantique Universités, LAMP, EA3825, Faculté des Sciences et des Techniques, 2 rue de la Houssinière - BP 9208, Nantes, F-44000 France.

Abstract

The optical properties of lead zirconate titanate (PZT) thin films deposited on ZnO were studied by m-lines spectroscopy. In order to retrieve the refractive index and the thickness of both layers from the m-lines spectra, we develop a numerical algorithm for the case of a two-layer system and show its robustness in the presence of noise. The sensitivity of the algorithm of the two-layer model allows us to relate the observed changes in the PZT refractive index to the PZT structural change due to the ZnO interface of the PZT/ZnO optical waveguide.

Key words: m-lines, composite waveguides, PZT
PACS:

1 Introduction

PZT ferroelectric thin films exhibit interesting optical properties, such as large electro-optic effects (Pockels, Kerr), a high refractive index, and a high transparency at visible and infra red wavelength. These properties are promising for the realization of different applications in the field of integrated optics as sensors or components for optical communications (optical shutter, waveguide, filter). In order to obtain active devices profiting from the electro-optic properties, electrodes

Email address: dominique.leduc@univ-nantes.fr (T. Schneider, D. Leduc, J. Cardin, C. Lupi, N. Barreau⋆ and H. Gundel).

have to be integrated. Most commonly they are made of transparent conductive materials like doped ZnO or indium tin oxide (ITO) when the absorption of light is a critical factor. The present paper studies a bilayer made of PZT and a transparent ZnO bottom electrode. It is generally known, that the crystallization behavior of ferroelectric thin films strongly depends on the structural properties of the substrate and hence may be influenced by the existence of an interface layer. This has been shown particularly for the case of PZT thin films elaborated on metal substrates using different conducting oxide interface layers [1]. In the case of the PZT/ZnO waveguide, we are interested in the relation between the PZT structural change and the optical properties of the films. For this purpose we developed a characterization method for a two layer planar waveguide based on prism coupler spectroscopy (or m-lines). M-lines spectroscopy [2,3,4] is widely used in order to determine the refractive index and the thickness of single layer homogeneous films. The refractive index profile of inhomogeneous waveguide can also be reconstructed with m-lines spectroscopy by using methods based on WKB approximation [5,6]. These methods are well suited in the case of guides where the index profile can be described by an a priori known continuous function. The case of multilayer guides where the index profile contains abrupt discontinuities, however, is less investigated. Dispersion equations of guided modes for the two layer guides were initially introduced by Tien [7] and several experiments were performed [8,9,10,11]. The reconstruction of the film parameters in these measurements were made with the help of an optimization method, the simplex algorithm in general, that minimizes the differences between the measured effective indices and the calculated ones from the dispersion equations. In our approach, we choose to directly solve the system of dispersion equations. This requires to determine the roots of a system of non linear equations with five unknowns (the refractive index and the thickness of the two layers and the order of the first mode in the spectrum). The first section of the present paper is devoted to the study of the efficiency of this method. We will especially examine the influence of the noise in order to estimate the accuracy of the results. Then in the second section, we will apply the method in order to firstly characterize the ZnO layer and secondly the two-layer waveguides.

2 Characterization of two layers films using m-lines spectroscopy

2.1 Two layer dispersion equations

The analysis of m-lines spectra requires to know the dispersion equation for the studied guide. Because of its compactness, the transfert matrix method [12] is well suited for analysing multilayer waveguides. The geometry of the guide is shown

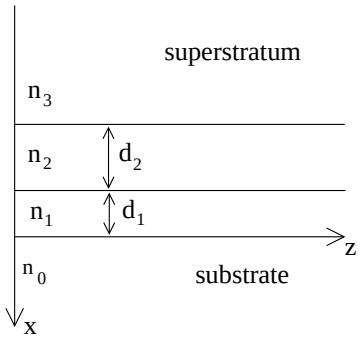

Fig. 1. Two layer waveguide.

in the figure 1. The layer j has a refractive index n_j and a thickness d_j. The layer 0 corresponds to the substrate and the layer 3 to the superstratum. In our case, $n_0 = 1.5169$ and $n_3 = 1$ at 632.8 nm wavelength. For TE modes, the electrical field in the layer j has only one component along the (Oy) axe : $E_{jy}(x,z) = A_j\,\mathrm{e}^{i\gamma x}\,\mathrm{e}^{i\beta_m z} + B_j\,\mathrm{e}^{-i\gamma x}\,\mathrm{e}^{i\beta_m z}$ and the tangential component of the magnetic field is $H_{jz} = i(\omega\mu_0)^{-1}\,\mathrm{d}E_{jy}/\mathrm{d}x$. In these expressions, ω is the angular frequency and β_m is the propagation constant of the m$^{\mathrm{th}}$ guided mode. It is usually written as $\beta_m = kN_m$, where k is the wavevector modulus in vacuum and N_m the effective index. The x component of the wavevector, γ_j, gives the nature of the waves in the layer j : $\gamma_j = k(\omega\mu_0)^{-1}\,|n_j^2 - N^2|^{1/2}$ for travelling waves and $\gamma_j = ik(\omega\mu_0)^{-1}\,|n_j^2 - N^2|^{1/2}$ for evanescent waves. In the following, we will call $a_j = k\,|n_j^2 - N^2|^{1/2}$.

A transfert matrix M_j is associated to each layer :

$$M_j = \begin{pmatrix} \cos(\omega\mu_0\gamma_j d_j) & \dfrac{i}{\gamma_j}\sin(\omega\mu_0\gamma_j d_j) \\ i\,\gamma_j \sin(\omega\mu_0\gamma_j d_j) & \cos(\omega\mu_0\gamma_j d_j) \end{pmatrix} \tag{1}$$

The tangential component of the electric and the magnetic fields E_y and H_z must be continuous at the interface to satisfy boundary conditions. These conditions and the condition for obtaining guiding lead to the equation :

$$\begin{pmatrix} 1 \\ -\gamma_3 \end{pmatrix} E_{3y} = M_2 M_1 \begin{pmatrix} 1 \\ \gamma_0 \end{pmatrix} E_{0y} = M \begin{pmatrix} 1 \\ \gamma_0 \end{pmatrix} E_{0y} \tag{2}$$

which has solutions only for :

$$\gamma_3 m_{11} + \gamma_3\gamma_0 m_{12} + m_{21} + \gamma_0 m_{22} = 0 \tag{3}$$

where m_{ij} are the components of the matrix M.

The refractive index of PZT is known to be higher than that of ZnO ($n_2 > n_1$). Two kinds of guided waves are possible in this case :

- guided waves in layer 2, evanescent waves in the other layers

$$a_2\, d_2 - \arctan\left(\frac{a_3}{a_2}\right) - \arctan\left[\frac{a_1^2 \tanh(a_1\, d_1) + a_0 a_1}{a_1 a_2 + a_0 a_2 \tanh(a_1\, d_1)}\right] - m\,\pi = 0 \qquad (4)$$

- guided waves in layer 1 and layer 2, evanescent waves in the substrate and in the superstratum

$$a_2\, d_2 - \arctan\left(\frac{a_3}{a_2}\right) + \arctan\left\{\frac{a_1}{a_2}\tan\left[a_1\, d_1 - \arctan\left(\frac{a_0}{a_1}\right)\right]\right\} - m\,\pi = 0 \qquad (5)$$

Equations 4 and 5 are the dispersion equations for the two layer waveguide.

2.2 Data analysis

The characterization of a two layer waveguide requires to determine 5 unknowns : the refractive indices and thicknesses of both layers and the order (m_1) of the first mode appearing in the m-lines spectrum. Very often, the latter parameter is neglected and the first mode in the spectrum is assumed to be the fundamental mode. The low order modes, however, are more difficult to excite since they require an high incidence angle and often spectra without the fundamental mode are observed. Therefore it seems indicated not to make any assumption on the order of the first mode and to consider it as an unknown. In order to determine all the unknowns, at least 5 modes in the m-lines spectrum have to be identified. In general, *ie* when the thicknesses of the layer 1 and layer 2 and the differences between the refractive indices of the different layers are large enough, a spectrum contains $M > 5$ modes.

One difficulty consists in associating the correct equation to each mode. As shown by equations 4 and 5, the effective index of a mode depends on the type of guiding, either in one or in two layers.Hence a rupture in the spectrum corresponding to the transition between these two types has to be determined. In the following we will call m_2 the order of the first guided mode in two layers. Given that the dispersion equations are transcendental, it is not possible to derive a general analytical expression for m_2. Numerical simulations with noisy datas, however, showed that m_2 is the value of m such that $|N_m - N_{m-1}| > |N_{m+1} - N_m|$ (see figure 2). This criterion results in a correct value of m_2 in the case of two thirds of the simulated waveguides. For almost all the other cases, the mismatch is equal to +1. Only one hundred

of simulations from more than two millions lead to different results. Then, in our data analysis protocol, we first assume that m_2 obeys the criterion stated above and try then to solve the dispersion equations. If the program does not converge, we substract one from the value of m_2 given by the criterion and again try to solve the equations. If this second step also fails, we may vary m_2 from 0 to M. It is observed that the program only converges in the case of the real value of m_2.

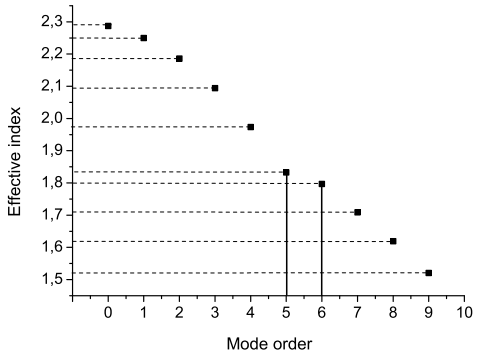

Fig. 2. Effective indices of the guided modes of a two layer film defined by $n_1 = 1.9$, $d_1 = 1$ μm, $n_2 = 2.2$ and $d_2 = 1.4$ μm.

In order to retrieve the thin films chatacteristics, we consider the 4 unknowns n_1, d_1, n_2 and d_2 and we varie m_1. The C_M^4 systems of 4 dispersion equations are solved with a Newton-Raphson algorithm. For each value of m_1, we obtain $C \leq C_M^4$ sets of solutions. The synchronous angles (ϕ_{calc}) corresponding to each solutions are calculated with a bisection algorithm and we compute the mean difference between these angles and the measured synchronous angles (ϕ_{meas}) :

$$\sigma(m_1) = \sqrt{\frac{\sum_{i=1}^{C}\sum_{j=0}^{M-1}(\phi_{ij}^{\mathrm{calc}} - \phi_j^{\mathrm{meas}})^2}{MC^2}} \tag{6}$$

The minimum of $\sigma(m_1)$ gives the correct indexation. Finally, the solutions are the mean values of the solutions corresponding to the right indexation.

2.3 Numerical tests

In order to estimate the accuracy of the numerical procedure described in the previous section, 10000 guides were simulated, n_1 varying from 1.8 to 1.98 and n_2 from 2.12 to 2.30 by steps of 0.02, d_1 varying from 0.6 μm to 1.05 μm and d_2

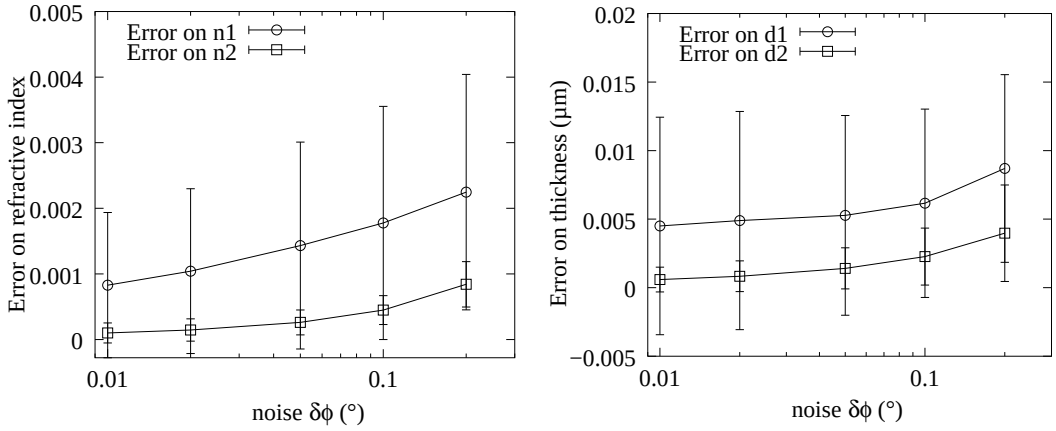

(a) Refractive index (b) Thickness

Fig. 3. Mean errors on the refractive index and the film thickness as a function of noise.

from 0.8 μm to 1.25 μm by steps of 50 nm. These ranges correspond to the values of the layers which we process. For each waveguide $\{n_1, d_1, n_2, d_2\}$, the set of synchronous angles $\{\phi^j_{\text{th}}\}$ is calculated and a noise randomly choosen in the range $[-\delta\varphi; \delta\varphi]$ is added in order to obtain a set of noisy synchronous angles $\{\phi^j_{\text{noisy}}\}$. This set is used as input data of the numerical procedure. In order to get a statistical estimate of the accuracy, 100 sets of noisy angles were studied for each guide. The influence of noise was evaluated by varying $\delta\varphi$ between 0.01° and 0.2°. The distributions of errors on the different parameters for one waveguide follow a normal law. So, for each waveguide we consider that the error on one parameter is the mean value of the errors over the 100 noisy sets. Highest errors arise for guides with the smallest index differences between the two layers and the smallest thicknesses. The effect of noise is shown in figure 3. The errors on the refractive indices are plotted in figure 3a and the errors on the thicknesses in figure 3b. The lengths of the errorbars is twice the standart deviation. The error on n_2 is smaller than the error on n_1 and does not exceed 1.10^{-3} in the considered noise range, whereas the error on n_1 is of the order of a few 10^{-3}. The thicknesses are expected to be determined with a precision of the order of 10 nm.

3 Characterization of PZT deposited on ZnO

3.1 Optical properties of the ZnO layer

Conducting transparent layers of Al doped ZnO in hexagonal phase were deposited by rf magnetron sputtering at room temperature. In our case, a heat treatment of

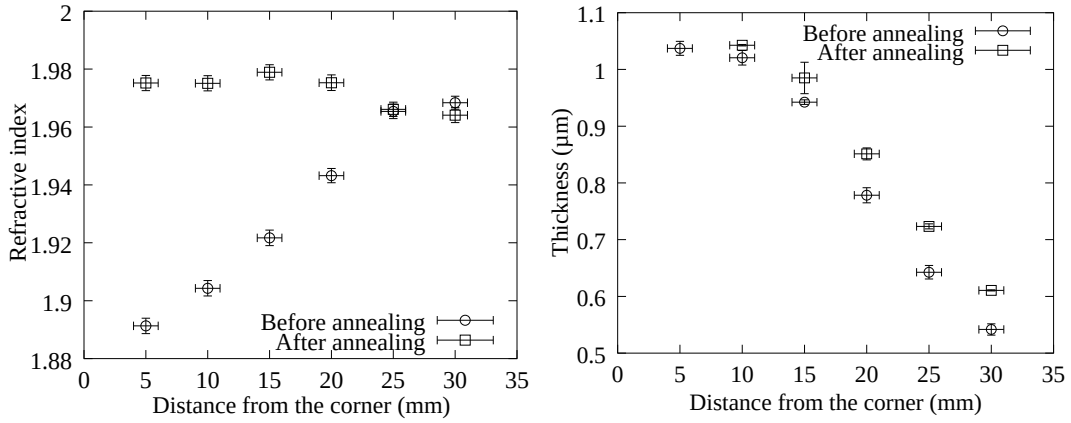

(a) Refractive index (b) Thickness

Fig. 4. Evolution of the refractive index and the film thickness along the diagonale of sample 1 before and after thermal annealing.

650°C is required for PZT cristallization in the perovskite phase. In order to evaluate the possible effects of this treatment, a preliminary study on the ZnO layers deposited on 25×25 mm Corning 1737F glass substrates was performed.

The zinc oxyde layers were grown by rf magnetron sputtering from a ϕ3" ZnO/Al_2O_3 (98/2 wt. %) ceramic target. Prior to the deposition, a base pressure lower than 5.10^{-7} mbar is reached and pure Ar is used as a sputter gas at a chamber pressure of 2.10^{-3} mbar during the deposition process. The applied rf power of 200 W results in a growth rate of approximatively 100 nm/min on axis at a target-substrate distance of 7.5 cm during 10 min. As four samples were grown at the same time, the substrates were shifted from the center of symetry of sputtering chamber, and the thickness of ZnO decreased along the diagonale of the substrate. The ZnO target contains 2 wt% of Al2O3, which corresponds to a [Al]/[Zn+Al] atomic ratio of about 3.3%. In order to investigate the aluminium content within the thin films, an electron dispersion spectroscopy (EDS, JEOL 5800 LV equipped with a X-ray detector) mapping was performed on thin films grown on a silicon wafer (aluminium/zinc-free substrate) with the same procedure than that used in the present work. The analysis showed that the aluminium content is homogeneous over the whole film surface and its value is 3.3%±0.5%.

The films were characterized with m-lines spectroscopy using a set-up and data analysis program described elsewhere [13]. The samples were measured as deposited at several points every 5 mm along the diagonale of the substrate. The evolutions of refractive index and thickness of sample 1 along this line are represented in the figure 4a and 4b (curves with circles). These curves reveal the inhomogeneity of the film due to the deposition technique. From one corner to another, the thickness decreases from 1.04 μm to 0.54 μm. Moreover it can be seen that the refractive

index increases from 1.89 to 1.97. This implies that the cristalline structure of the ZnO is not the same across the film. The other samples show the same behavior, but sometimes, the measurements at the lower thicknesses were difficult because of the lack of modes when the thickness becomes too small.

After this first characterization, the films were annealed at 650°C during 3 min and cooled slowly in the oven during 3 hours. The results of the index and thickness of sample 1 are also shown in the figures 4a and 4b (curves with squares). Obviously, the rapid thermal annealing does not change significantly the thickness, however, it homogenizes the refractive index of the film. Indeed, after annealing, the index ranges between 1.975 ± 2.10^{-3} and 1.964 ± 1.10^{-3}. Previous studies [14,15,16,17] pointed out that the annealing improves the crystallinity of the ZnO films by promoting the formation of stoichiometric ZnO. The increase of the intensity and the decrease of the FWHM of the diffraction peak (xyz) well illustrate this phenomenon (see figure 5). Hence, the modification of refractive index with annealing can be related to this crystallinity improvement.

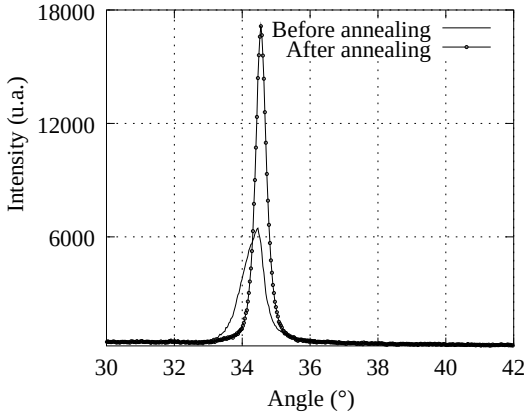

Fig. 5. X-ray diffraction diagramm of the ZnO film (sample 1) before and after annealing.

3.2 Optical properties of two layers waveguides

PZT 36/64 thin films were elaborated by Chemical Solution Deposition technique and were spin-coated on the ZnO layer at 2000 rpm for samples 1 to 3 and 1000 rpm for samples 4 and 5. A modified sol-gel process was used for the elaboration of the precursor solution, which consisted of lead acetate dissolved in acetic acid, zirconium and titanium n-propoxide; ethylene glycol was added in order to prevent from crack formation during the annealing process. The deposited films were dried on a hot plate and a Rapid Thermal Annealing procedure at 650°C resulting

in the formation of a polycrystalline perovskite phase as shown by the XRD pattern (figure 6). The samples were also studied with scanning electron microscopy.

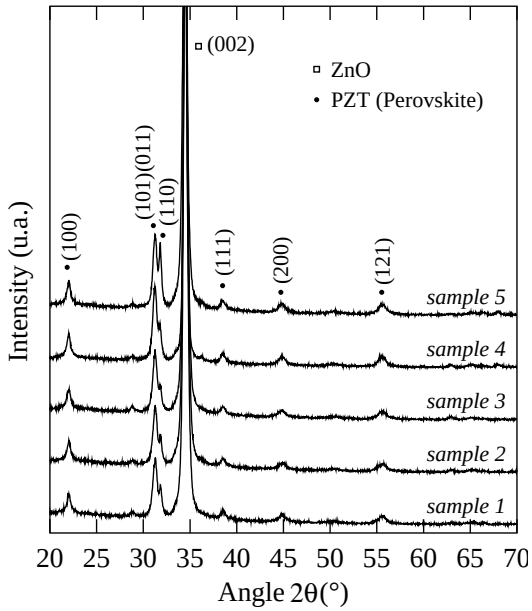

Fig. 6. X-ray diffraction diagramm of the two layer films.

An example is shown in figure 7. The two layer structure appears clearly on this

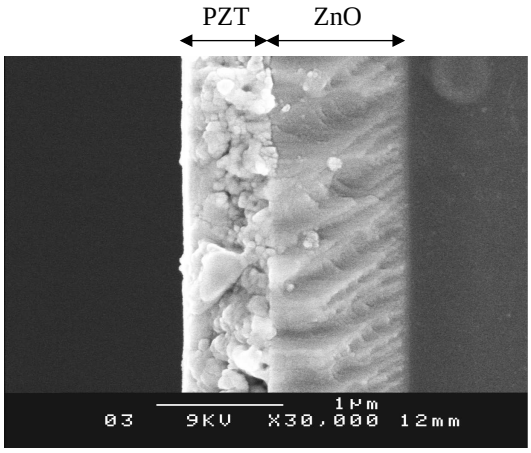

Fig. 7. SEM photography of sample 3.

photography. The thickness of the ZnO layer is approximatively 1.1 μm and the thickness of the PZT layer is close to 0.7 μm. The values are in agreement with the elaboration process.

The films were measured with m-lines at several points along the diagonale of the sample. As an example, the spectrum of sample 5 is shown on figure 8. The narrow

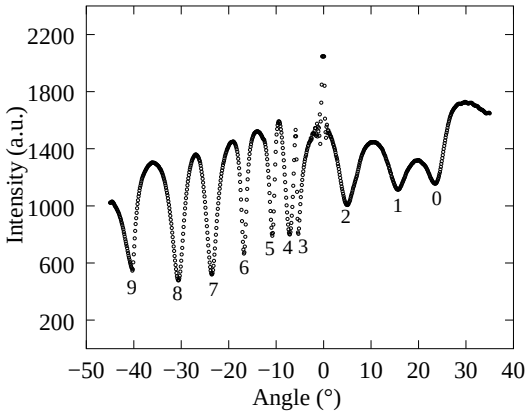

Fig. 8. M-lines spectrum measured at one corner of sample 5.

Table 1
Comparison of the measured and the calculated synchronous angles.

modes	1	2	3	4	5	6	7	8	9
measured (°)	23.5	15.60	4.90	-5.30	-7.20	-10.80	-16.70	-23.40	-30.40
calculated (°)	23.8	15.58	5.07	-5.28	-7.19	-10.75	-16.87	-23.54	-30.52

peaks correspond to the waves guided in two layers while the broad peaks correspond to waves guided in the PZT layer only. The broadening is not a peculiarity of the two layer structure, it can be also observed with PZT single layers and is probably due to the diffusion of light. The measurement given in figure 8 was analysed with the previously described procedure. Only the modes 4 to 8 were considered which can be located with a precision of $\pm 0.05°$, while the uncertainty on the position of the first modes is of the order of 0.5° because of the broadening. From this measurement we obtain : $n_1 = 1.977 \pm 9.10^{-3}$ and $d_1 = 1.11 \pm 4.10^{-2}\ \mu m$ for the ZnO layer and $n_2 = 2.36 \pm 4.10^{-2}$ and $d_2 = 1.01 \pm 7.10^{-2}$ for the PZT. In order to verify the exactness of the results, the values may be injected in the dispersion equations 4 and 5. Synchronous angles in very good agreement with the measured angles are found (see Table 1). The differences never exceed 0.3°, corresponding to a maximum difference between measured and calculated effective indices of the order of 10^{-3}.

The results obtained with other samples are summarized in the figure 9. It was not possible to analyze each measurement, especially those corresponding to points where the ZnO layer was too thin. Everywhere else a good agreement between the refractive indices and thicknesses of the ZnO determined from the single and the double layers was obtained. The variation is of the order of 10^{-2} for the index and 100 nm for the thickness in the worst case but in general remains lower than the uncertainties.

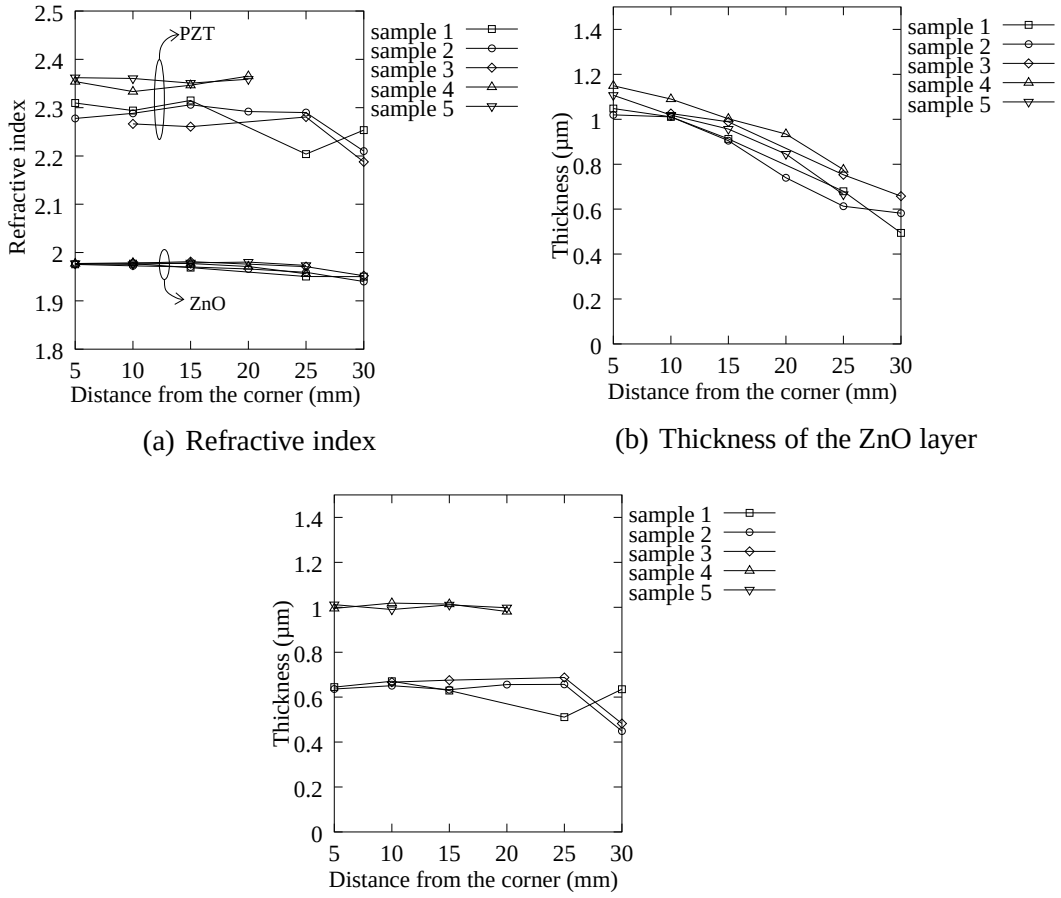

(a) Refractive index

(b) Thickness of the ZnO layer

(c) Thickness of the PZT layer

Fig. 9. Evolution of the refractive index and the film thickness along the diagonale of the two layer samples.

The measurement of the PZT refractive index reveals the influence resulting from the ZnO interface layer. A PZT film of the identical precursor composition, directly spin-coated on the glass substrate, has a refractive index close to 2.23, whereas the refracting index of the PZT deposited on ZnO is higher as can be seen in the figure 9a. Moreover, the index varies from close to 2.36 for the thicker PZT films (deposited at 1000 rpm) to close to 2.30 for the thinner films (deposited at 2000 rpm). This indicates that the structure of the film might be different. In order to verify this assumption, we compare in figure 10, XRD measurements for the two cases. The unique peak at 2θ=31° for PZT deposited on glass, corresponding to a rhomboedric structure is doubled when spin-coating the same composition PZT 36/64 on ZnO, indicating the appearance of a second phase corresponding to the tetragonal PZT structure.

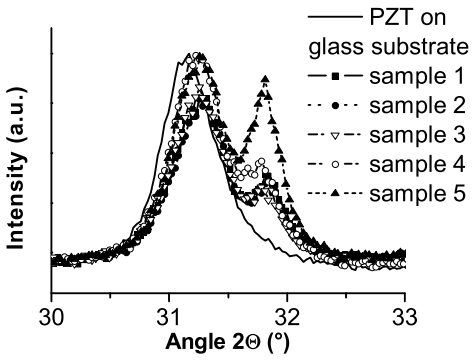

Fig. 10. X ray diffraction diagramms

4 Conclusions

A two-layer PZT/ZnO wave-guide structure has been elaborated by rf magnetron sputtering and chemical solution deposition technique. The numerical tools for analyzing the m-lines spectra obtained from this two-layer system were developed and their efficiency in the presence of noise was demonstrated. In the case of a single ZnO layer, the benefice of a heat treatment at higher temperatures in terms of homogenization of the refractive index has been shown. The study of the PZT thin films revealed the sensitivity of the m-lines characterization method. The different crystallization behavior of the ferroelectric resulting from the different structural properties of the underlying layers (glass or ZnO), could be observed by m-lines spectroscopy as a change of the PZT refractive index. This appears to be very important for the design of single mode waveguides since the thickness of the guiding layer is related to the difference between the refractive indices of the guiding and the confining layers. The presented work can be considered as a first step towards the characterization of three layer composite structures by m-lines spectroscopy, also resulting in the possibility to determine the refractive index as a function of an applied electric field and to deduce the electro-optical coefficient.

References

[1] R. Seveno H. W. Gundel and S. Seifert, Applied Physics Letters 79 (2001) 4204.

[2] P. K. Tien and R. Ulrich, Journal of the Optical Society of America 60(10) (1970) 1325.

[3] R. Ulrich, Journal of Optical Society of America 60(10) (1970) 1337.

[4] R. Ulrich and R. Torge, Applied Optics 12(12) (1973) 2901.

[5] J. M. White and P. F. Heidrich, Applied Optics 15 (1976) 151.

[6] K. S. Chiang, Journal of Lightwave Technology 3 (1985) 385.

[7] P.K. Tien, R.J. Martin, and G. Smolinsky, Applied Optics 12(8) (1973) 1909.

[8] W. Stutius and W. Streifer, Applied Optics 16(12) (1977) 3218.

[9] M. Matyáš J. Bok, and T. Sikora, Physica Status Solidi (a) 126 (1991) 533.

[10] J. Aarnio, P. Kersten, and J. Lauckner, IEE Proc. Optoelectron. 142(5) (1995) 241.

[11] E. Auguściuk and M. Roszko, Proceedings of SPIE 5451 (2004) 495.

[12] J. Chilwell and I. Hodgkinson, Optical Society of America Journal A 1 (1984) 742.

[13] J. Cardin, D. Leduc, T. Schneider, C. Lupi, D. Averty, and H.W. Gundel, Journal of the European Ceramic Society 25(12) (2005) 2913.

[14] X. W. Sun and H. S. Kwok, Journal of applied physics 86(1) (1999) 408.

[15] Y. Ohya, H. Saiki, and Y. Takahashi, Journal of Materials Science 29 (1994) 4099.

[16] N. Mehan M. Tomar V. Gupta and A. Mansingh, Optical Materials 27 (2004) 241.

[17] R. Al Asmar, G. Ferblantier, F. Mailly, P. Gallborrut, and A. Foucaran, Thin Solid Films 473 (2005) 49.